

## Formation of surface superstructures by heat treatments on Ni-contaminated surface of Si(110)

T. Ichinokawa, H. Ampo, S. Miura, and A. Tamura

*Department of Applied Physics, Waseda University, 3-4-1 Ohkubo, Shinjuku-ku, Tokyo 160, Japan*

(Received 21 August 1984; revised manuscript received 14 December 1984)

On clean and Ni-contaminated surfaces of Si(110), experiments of low-energy electron diffraction (LEED) and Auger-electron spectroscopy (AES) were carried out under various heat treatments. The Si(110) clean surface has a "16×2" structure and it transforms reversibly to 1×1 at 740°C. On the other hand, Ni-contaminated surfaces exhibit several surface superstructures at room temperature, e.g., the 4×5, 2×1, and 5×1, depending on the heat treatments. Moreover, it is found that these structures are closely correlated with Ni concentration at the surface. Quantitative Auger-electron analyses show that a thickness of the Ni-contaminated layer varies from several angstroms to 20 Å and the surface Ni concentration changes from 7% to 1%, depending on the heat treatment. These variations give rise to changes of the surface superstructure depending on the heat treatment.

### I. INTRODUCTION

It was reported by Jona<sup>1</sup> that a Si(110) clean surface has various reconstructed structures, e.g., the 4×5, 2×1, 5×1, 9×1 (or 7×1), "X" and "initial," depending on the relevant heat treatments. Olshanetsky and Shklyayev<sup>2</sup> observed similar structures and suggested a possibility that the existence of various structures on the clean Si(110) surface after the heat treatments is the consequence of reversible order-order phase transitions which take place at certain temperatures. These structures were also observed by Hagstrum and Becker<sup>3</sup> and Sakurai *et al.*<sup>4</sup> However, it was reported recently that low-energy electron-diffraction<sup>5</sup> (LEED) and reflection high-energy electron-diffraction<sup>6</sup> (RHEED) experiments on the clean Si(110) surface show a unique reconstructed structure pattern composed of a set of superspot rows parallel to the  $\langle\bar{1}11\rangle$  direction, referred to as a Si(17 15 1)2×1 structure by Olshanetsky and Shklyayev.<sup>2</sup> Yamamoto and Ino<sup>6</sup> named this structure as "16×2" structure, disregarding a rotation of unit meshes between fundamental and reconstructed structures. This notation is adopted in the present paper for convenience.

Consequently, the cause of the formation of various reconstructed structures reported by Jona<sup>1</sup> and Olshanetsky and Shklyayev<sup>2</sup> is still in controversy. Therefore, the analysis of formation of the reconstructed structures on Si(110) is very interesting.

### II. EXPERIMENTAL APPARATUS AND PROCEDURES

A high-vacuum chamber capable of reaching  $2 \times 10^{-10}$  Torr and equipped with a cylindrical mirror analyzer (CMA) and a LEED optics was used. After the Si(110) surface was chemically etched by etching solution (HNO<sub>3</sub>:HF:CH<sub>3</sub>COOH concentrations in the proportion 4:1:2), the sample was put in the high-vacuum chamber with Teflon forceps and heated by direct electric current up to 1000°C. Surface temperature was measured by a thermocouple calibrated with an optical pyrometer. A Si(110) clean surface was obtained with impurity Auger

signals (O, C, and Ni) less than  $\frac{1}{2000}$  of that of Si LVV.

The Ni-contaminated surfaces were prepared initially by rubbing the specimen surface with stainless-steel forceps or a nickel rod, or by Ni vacuum evaporation on the clean surface. Afterward, the specimens were heated up to temperatures higher than 1000°C. We used these as initial samples of Ni-contaminated surfaces for successive heat treatments.

Auger-electron spectra were measured with a CMA at primary energies  $E_p = 2-3$  keV, and LEED patterns were observed at  $E_p = 30-100$  eV with varying heat treatment. The Auger-electron spectra were obtained with a lock-in amplifier in the first derivative mode and the semiquantitative analyses were carried out on a peak-to-peak height using suitable sensitivity factors.<sup>7</sup> The ratios of Ni-LMM to Si LVV yield for the Ni-contaminated surfaces were found to be in a range from few percent to less than 1%, depending on the heat treatment.

### III. EXPERIMENTAL RESULTS

#### A. Si(110) clean surface

The LEED pattern of the "16×2" structure seems to be the same as the Si(17 15 1)2×1 structure reported by Olshanetsky and Shklyayev.<sup>2</sup> The 16×2 structure observed by LEED in the present experiment transforms into a 1×1 structure at 740°C. Furthermore, intensities of the superstructure spots decrease appreciably at 640°C. These facts agree with RHEED results by Yamamoto and Ino,<sup>6</sup> except for the temperature difference of the phase transitions. Our results are lower than those of Yamamoto and Ino by about 60°C. The phase transitions are reversible and the temperature range of the phase transitions spreads over 30–40°C.

#### B. Ni-contaminated surface of Si(110)

Ni-contaminated surfaces of Si(110) prepared by methods described above show the 4×5 structure after annealing at temperature higher than 1000°C. The 4×5

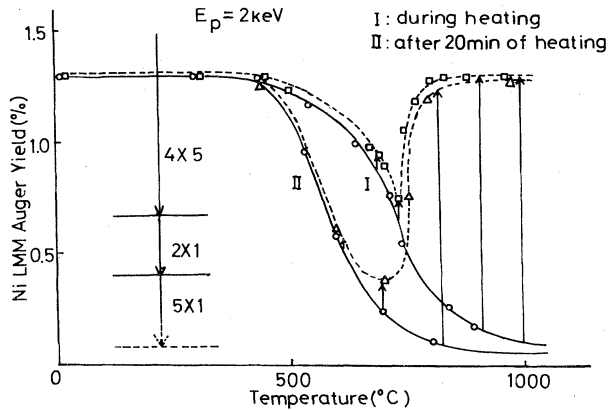


FIG. 1. Variations of Auger-electron yield of Ni *LMM* with increasing temperature (solid curves) and after rapid cooling from annealing temperature to room temperature (dashed curves). I, during heating; II, after 20 min of heating at each temperature.

structure changes into the  $2 \times 1$  and  $5 \times 1$  structures at approximately 700 and 750°C, respectively, as temperature increases. The surface Ni concentration of the contaminated layer was measured as a function of annealing temperature and annealing time. The surface concentration decreases rapidly with increasing temperature in a range higher than 500°C as shown by solid curves in Fig. 1. Curve I represents the Ni Auger yield measured with increasing temperature and curve II that after 20 min of annealing at each temperature.

The surface Ni concentration depends not only on the annealing temperature but also on the annealing time at each temperature. The variations of the surface Ni concentration with annealing time are shown in Fig. 2 at various temperatures. The Ni Auger yield decreases rapidly with increasing temperature and is almost constant in the temperature range lower than 500°C. These facts suggest that Ni impurities at the surface diffuse into the bulk at temperature higher than 500°C and the thickness of the Ni-contaminated layer increases with temperature.

On the other hand, by rapid cooling at a speed of several seconds from annealing temperatures to 300°C, the surface Ni concentration at room temperature in-

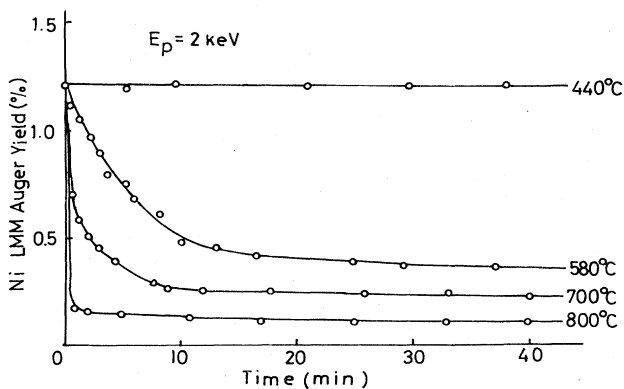


FIG. 2. Variation of Auger-electron yield of Ni *LMM* with annealing time at various temperatures.

creases as shown by broken curves in Fig. 1, depending on annealing temperature and annealing time. In the case of the rapid cooling from temperatures higher than 800°C, the surface Ni concentration recovers the initial value before the heat treatment. The cooling from temperature between 600 and 800°C, however, does not result in recovery to the initial value and forms lower Ni concentration layers at the surface as shown in Fig. 1. By rapid cooling after a long time annealing at 700°C, a minimum value of the Ni Auger yield was obtained. The LEED patterns of the  $4 \times 5$ ,  $2 \times 1$ , and  $5 \times 1$  structures appeared, depending on the relevant heat treatments and were closely correlated to the surface Ni concentration. Thus, the way in which surface structures appear at room temperature is determined uniquely by heat treatments.

In the present experiments, it was found that for the surface contaminated by rubbing with stainless-steel forceps, only a Ni-impurity signal was detected all over the surface after annealing at temperatures higher than 1000°C, but no other elements were detectable. This phenomenon is understood by way of the following experimental consideration. A number of metals (e.g., Ni, Fe, and Cr) form a silicide layer on a Si surface by annealing at temperature higher than 600°C after vacuum evaporation over several monolayers. Most silicide layers are vaporized by successive annealing at temperature higher than 1000°C and afterward a clean surface of the substrate appears. But, in the case of Ni silicide, a surface contaminated by Ni with a concentration of less than few percent remains after the evaporation of the Ni silicide and is very hard to remove even after annealing to temperatures higher than 1200°C. This fact indicates that the Ni-contaminated layer of concentration of a few percent is stable on the Si surface and difficult to remove even after high-temperature annealing. Similar behaviors were also observed for Co-contaminated surfaces on Si(110). The results will be reported elsewhere.

#### IV. DISCUSSION

The result of Fig. 1 suggests that thickness and surface concentration of the Ni-contaminated layer vary with heat treatment. The thickness increases with annealing temperature beyond 500°C and decreases upon rapid cooling. The Ni impurity segregates to the surface with rapid cooling. It recovers the initial concentration by rapid cooling from temperatures higher than 800°C, but it cannot do so from temperatures lower than 800°C because a diffusion coefficient towards the surface decreases with temperature. The solubility of Ni within Si is  $10^{-4}$ – $10^{-6}$  in the temperature range from 600 to 1200°C. High Ni concentrations of  $10^{-2}$ – $10^{-3}$  are not stable within the bulk, hence a thick contaminated layer at high temperature should be segregated to the surface upon rapid cooling. Segregation of high-atomic-number impurities to grain boundaries or crystal imperfections has been investigated by many workers<sup>8–10</sup> for Si crystals. The mechanism of the surface segregation observed by the present experiment is probably similar to that toward grain boundaries.

To estimate the thickness of the Ni-contaminated layer, Ni Auger-electron signals of different energies were uti-

TABLE I. Ratios of Auger-electron yields between different transitions of Ni and between Ni *LMM* and Si *LVV* for surface structures,  $4 \times 5$ ,  $2 \times 1$ , and  $5 \times 1$ .  $E_p = 3$  keV. Ni *LMM* (847 eV), Ni *MVV* (61 eV), and Si *LVV* (92 eV).

Ratios	Structures ( <i>i</i> )		
	1 $4 \times 5$	2 $2 \times 1$	3 $5 \times 1$
$I_{\text{Ni MVV}}/I_{\text{Ni LMM}}$	1.2	1.0	0.8
$I_{\text{Ni LMM}}/I_{\text{Si LVV}}$	1.9	1.3	1.0

lized. The peak ratios between different transitions of Ni,  $I_{\text{Ni MVV}}(61 \text{ eV})/I_{\text{Ni LMM}}(847 \text{ eV})$ , vary with the surface structures as shown in Table I, because the thickness and concentration of these diffusion layers and escape depth of Auger electrons of different energies are different. To estimate the ratios, the effect of superposition of a second-order bulk-plasmon-loss peak of Si *LVV* (92 eV) upon the Ni *MVV* peak (61 eV) was eliminated by referring to a spectrum of the Si clean surface. The Auger-electron yield  $I_{ai}$  of *i* transition of an element *a* is expressed by<sup>11</sup>

$$I_{ai} = AI_p C_a \rho \lambda_{ai} B \sigma \omega_A RT, \quad (1)$$

where *A* is the area irradiated by the primary beam ( $\text{cm}^2$ ),

$I_p$  is the current density of the primary beam ( $\text{A}/\text{cm}^2$ ),  $\rho$  is the atomic density of the specimen ( $\text{atoms}/\text{cm}^3$ ),  $C_a$  is the concentration of element *a* (%),  $\lambda_{ai}$  is the escape depth (cm), *B* is the backscattering factor ( $> 1$ ),  $\sigma$  is the ionization cross section ( $\text{cm}^2/\text{atom}$ ),  $\omega_a$  is the Auger transition probability, *R* is the surface-roughness factor, and *T* is the transmission factor of the analyzer. Among the factors in Eq. (1),  $\sigma$  and  $\omega_A$  are determined for the relevant Auger transitions and  $C_a$  depends on the thickness of the diffusion layer. Other factors are regarded as constants under the same experimental condition. It is assumed here that the diffusion layer of state 1 (e.g., the  $4 \times 5$  structure) has a homogeneous concentration of  $C_{\text{Ni}}^1$  with a thickness  $z_1$ . To estimate the thickness and concentration for the  $4 \times 5$ ,  $2 \times 1$ , and  $5 \times 1$  diffusion layers (suffixed at  $i = 1, 2$ , and  $3$ , respectively), the following equations are available, taking into account the escape depth, thickness of the diffusion layers, and a take-off angle  $\theta$  ( $\theta = 42.3^\circ$ ) toward the CMA window:

$$\frac{I_{\text{Ni MVV}}^i}{I_{\text{Ni LMM}}^i} = \frac{\sigma \omega_A(\text{Ni MVV}) \int_0^{z_i} \exp(-z/\lambda_{\text{Ni MVV}} \cos \theta) dz}{\sigma \omega_A(\text{Ni LMM}) \int_0^{z_i} \exp(-z/\lambda_{\text{Ni LMM}} \cos \theta) dz} \quad (2)$$

and

$$\frac{I_{\text{Ni LMM}}^i}{I_{\text{Si LVV}}^i} = \frac{C_{\text{Ni}}^i \sigma \omega_A(\text{Ni LMM}) \int_0^{z_i} \exp(-z/\lambda_{\text{Ni LMM}} \cos \theta) dz}{\sigma \omega_A(\text{Si LVV}) \lambda_{\text{Si LVV}} \cos \theta} \quad (3)$$

Using the experimental values in Table I and setting

$$\sigma \omega_A(\text{Ni MVV})/\sigma \omega_A(\text{Ni LMM}) = 2.6,$$

$$\sigma \omega_A(\text{Ni LMM})/\sigma \omega_A(\text{Si LVV}) = 0.13,$$

$\lambda_{\text{Ni LMM}}(847 \text{ eV}) = 17 \text{ \AA}$ ,  $\lambda_{\text{Ni MVV}}(61 \text{ eV}) = 4 \text{ \AA}$ , and  $\lambda_{\text{Si LVV}}(92 \text{ eV}) = 4 \text{ \AA}$ , using values of data collections,<sup>7,11</sup> the thickness  $z_i$  and concentration  $C_{\text{Ni}}^i$  were calculated by Eqs. (2) and (3), respectively. The results are shown in Table II for the three structures. To check these values, the total mass of Ni impurities is compared among the three structures. The calculated mass ratio  $m_1:m_2:m_3$  equals 5.6:4.8:4.7 and is not precisely constant. The discrepancy may come from the assumption that the

TABLE II. Thickness and concentration of the surface Ni-contaminated layers for three structures,  $4 \times 5$ ,  $2 \times 1$ , and  $5 \times 1$ .

Structures	Thickness ( $\text{\AA}$ )	Concentration (%)
$4 \times 5$	8	7
$2 \times 1$	12	4
$5 \times 1$	18	2.6

surface-contaminated layer is homogeneous or from uncertainty of values of Auger transition probabilities. The Ni concentrations shown in Fig. 1 and Fig. 2 were corrected only with the sensitivity factors  $S_{ai}$  by setting  $S_{\text{Ni LMM}}/S_{\text{Si LVV}} = 0.44/0.45 \approx 1.7$ . Therefore, these values should be replaced by quantitative ones calculated by Eq. (3).

The Ni impurities introduced locally by rubbing with stainless-steel forceps diffuse all over the surface by annealing at temperatures higher than  $600^\circ\text{C}$ , but Fe and Cr in the stainless steel do not exhibit similar behavior as Ni. Furthermore, the Ni-contaminated layer is difficult to remove even after the high-temperature annealing, unlike other elements. Investigations to make the different properties of Ni clear from other elements on Si surface are in progress. The present authors are also interested in the formation of surface superstructures induced by impurities of low concentration.

The Si(111) surface forms a  $\sqrt{19} \times \sqrt{19}$  structure by Ni contamination as reported by Taylor<sup>12</sup> and Van Bommel and Meyer.<sup>13</sup> The kinetics of Ni-contaminated layers on other crystal planes by heat treatments is similar to those on Si(110), though not as many superstructures appear as on Si(110).

## V. CONCLUSION

The cause of the formation of various reconstructed structures by heat treatments on Si(110) is made clear on the basis of the effect of surface Ni contamination. The different properties of Ni from other elements at the Si surface are also pointed out, e.g., surface diffusion, formation of the surface superstructures, and removal of surface impurities by heat treatment.

## ACKNOWLEDGMENTS

The present studies were supported by a Grant-in-Aid for Science Research from the Ministry of Education (Japan) and by the Yamada Scientific Foundation. The present authors thank Dr. Yamamoto of Tohoku University for valuable discussions. Si(110) crystals were provided by the Toshiba Research and Development Center.

<sup>1</sup>F. Jona, IBM J. Res. Dev. 9, 375 (1965).

<sup>2</sup>B. Z. Olshanetsky and A. A. Shklyayev, Surf. Sci. 67, 581 (1977).

<sup>3</sup>H. D. Hagstrum and G. E. Becker, Phys. Rev. B 8, 1580 (1973).

<sup>4</sup>T. Sakurai, K. C. Pandey, and H. D. Hagstrum, Phys. Lett. 56A, 204 (1976)

<sup>5</sup>T. Oyama, S. Ohi, A. Kawazu and G. Tominaga, Surf. Sci. 109, 82 (1981).

<sup>6</sup>Y. Yamamoto and S. Ino (unpublished).

<sup>7</sup>*Auger-Electron Spectra Catalogue* (a data collection of elements) (ANELVA, Tokyo, 1979).

<sup>8</sup>M. Yoshida and K. Saito, Jpn. J. Appl. Phys. 6, 573 (1967).

<sup>9</sup>E. Nes. Acta Metall. 22, 81 (1974).

<sup>10</sup>G. Das, J. Appl. Phys. 44, 4459 (1974).

<sup>11</sup>P. W. Palmberg, in *Electron Spectroscopy*, edited by D. A. Shirley (North-Holland, Amsterdam, 1972).

<sup>12</sup>N. J. Taylor, Surf. Sci. 15, 169 (1969).

<sup>13</sup>A. J. Van Bommel and F. Meyer, Surf. Sci. 8, 467 (1967).